Subhorizontal Well Architecture Enhances Heat Production The Cachan Milestone

Pierre UNGEMACH, Miklos ANTICS and Mélanie DAVAUX

GPC Instrumentation Process (GPC IP) and Geofluid

165, rue de la Belle Etoile - Bât. 4A - BP 57072

95947 ROISSY CDG Cedex, France

pierre.ungemach@geoproduction.fr

Keywords: Geothermal energy, Well architecture, Directional drilling, Horizontal well logging & testing, Formation evaluation.

ABSTRACT

Complex reservoir settings, located in several European tectonised and multilayered – continental rift and sedimentary basin environments, have raised a demand among geothermal operators towards well designs capable of sustaining high productive capacities and prolonged thermal life.

The problematic however become more acute when contemplating, lower than anticipated, reservoir permeabilities, which require relevant, preferably innovative, well architectures to be substituted for long prevailing conventional drilling/completion practice.

Such issues are addressed by the subhorizontal well (SHW) concept, advocated as a means for mining heat from reservoir systems which would otherwise remain unchallenged, and field validated on a geothermal district heating (GDH) site south of Paris, France, in a stratified carbonate reservoir environment. The extended reach SHW trajectory aims at intercepting over a near 90° (in fact 85 to 95°, dip dependant) inclination the whole of the layered reservoir sequence, thus maximizing reservoir exposure area and well productivity. As a result, the concept may be regarded as intermediate between the horizontal and multilateral well architectures currently practiced by the oil industry. First of its kind in geothermal design engineering it however complies with the well completion and flow ratings specific to geothermal production standards.

The paper highlights the SHW doublet outcome with respect to directional RSS (Rotary Steerable System) drilling, logging while drilling (LWD), geochemically (X Ray Fluorescence, XRF and Difractometry, XRD) assisted geosteering and 1 000 m long drain stimulation logging and testing.

Extension of the technology to wider lateral investigation of reservoir attributes, assessment of depositional features (diagenetis, micro fracturing) driving reservoir porosity/permeability trends are also discussed.

1. INTRODUCTION

The SHW concept, first presented at the 36th Stanford Geothermal Reservoir Engineering Workshop (Ungemach et al, 2011) and further developed at the 2013 and 2016 European Geothermal Congress (Promis et al, 2013; Ungemach et al, 2016) is raising growing interest among geothermal operators since its successful achievement on a Paris Basin GDH site.

Here, the multi doublet heat extraction scheme faces three major, often critical, concerns (i) the replacement of aging, when not damaged, well infrastructures and productive/injective capacities, (ii) doublet densities approaching in several areas overpopulation, source of potential mining disputes, limiting well replacement opportunities and clouding new development issues, as a consequence of space restrictions and thermal breakthrough/reservoir cooling shortcomings, and, last but not least (iii) heat reclamation from locally moderately to poorly productive reservoir areas remaining unchallenged unless appropriate, field proofed, well architectures be made available.

Prior to this recent interest from geothermal operators long committed to conservatism, several milestones, along the SHW design are worth to mention. Bruel (2008) has suggested horizontal well trajectories as an alternative to conventional directional drilling applied to GDH doublets in the Paris Basin, assuming a single layer geothermal reservoir. Noteworthy also are the first horizontal wells completed at Schlattingen in the Swiss Canton of Thurgau. Not designed as such beforehand, the borehole was sidetracked as a remedial to the former vertical trajectory which proved almost dry. Incidentally the two fold kick off profile described by Frieg (2014) evidenced the need for incorporating wellbore stability calculations in the well design process.

Of interest to the project were the modern technological ingredients successfully implemented by several operators involved in the development of the deep seated targets hosted by a karstified limestone in the Southern Molasse Bavarian Basin (Münich area). Here, incorporation of 3D seismics, RSS (Rotary Steering Systems), LWD (Logging While Drilling) assisted geonavigation have secured high drilling success ratios reported by Mirjolet (2014), and are becoming a standard in exploring and producing such "risky" objectives (Schubert, 2015). The present paper, further to a description of the SHW architecture and accompanying geosteering drilling/navigation technology, will focus on the wireline logging, well testing and geochemical monitoring attributes of the well and reservoir assessment strategy. Results are discussed in the light of upgraded reservoir exposure/well performance issues, extended to a comprehensive review of a carbonate platform lithofacies, diagenetic, cements and microfracturing trends.

Technical and economic aspects are analysed in fine with a view to standardising the process in geothermal engineering.

2. SITE SELECTION AND WELL ARCHITECTURE

The site (Cachan) selected for the first implementation of the concept meets most of the afore mentioned GDH constraints i.e. a densely populated (sub)urban district, limited space availability, proximity of neighbouring, operating and commissioned doublets/triplets including two, 34 years old first generation completed wells exemplified in Figure 1 lease map, to which should be added locally moderate reservoir properties (15 to 10 Dm transmissivities), saturated production capacities (350 m3/h cumulated by two existing doublets) and poor system COP (ratio of yearly produced heat over consumed pumping power close to 9). The geothermal target is hosted by the Dogger (Mid-Jurassic) multilayered oolitic carbonates reservoir at a ca 1 600 mTVD depth.

The foregoing made this site eligible to innovative well designs securing technically and cost effective exploitation.

The project replaces two doublets, serviced since years 1984 and 1985, extending its productive capacities from 350 m^3/h – 45 000 MWhth/yr to 450 m^3/h – 60 000 MWhth/yr, ambitioning a COP of 20 instead of the former 9 MWhth/MWhel.

Well design conforms to the well path sketched in Figure 2, which shapes as a compromise between single horizontal and multilateral well profiles since the planned SHW trajectory intercepts the whole multilayered reservoir sequence, thus cumulating its individual layer flow contributions. Hence, given a thin layered reservoir setting and a long legged drain, the latter would, in most instances, trend near horizontal and recover accordingly significantly larger flow amounts compared to a standard deviated well design.

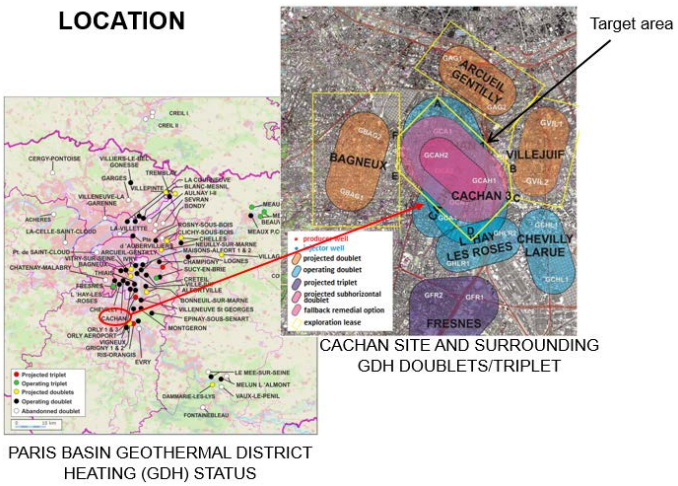

Figure 1: Site location and neighbouring GDH systems.

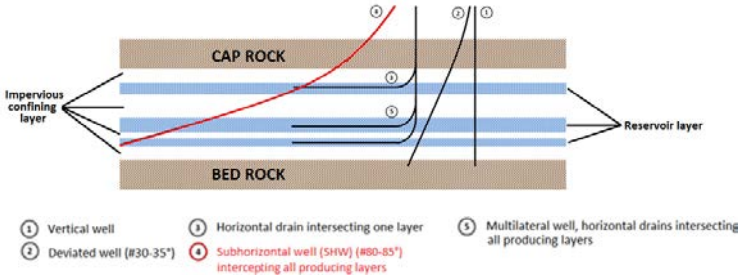

Figure 2: Subhorizontal well concept.

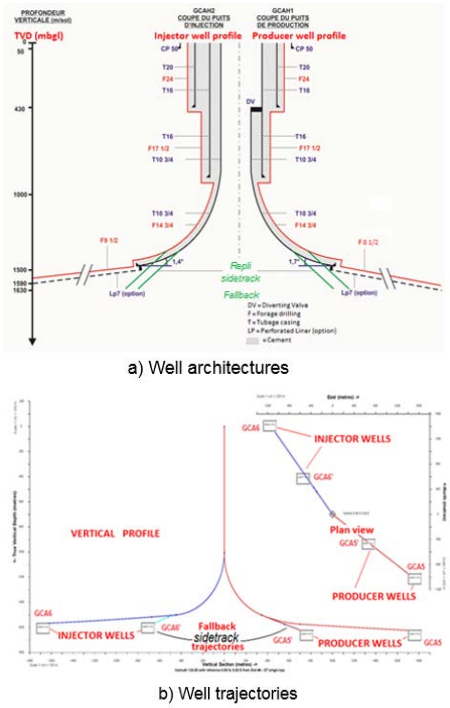

Figure 3: Subhorizontal well architectures and trajectories

3. DRILLING

Drilling mobilised a 350 t, electrically driven, heavy duty rig force on the existing heat plant (operated during works) and clustered well site. Both wells, quasi identical in design, include a dual drilled (18"1/2)/cased (16") vertical section followed by a deviated section initiated by a 14"3/4 in arc path, further 10"3/4 cased, achieved via a standard MWD (Measurement While Drilling) x PDM (Positive Displacement Motor) assembly and finalised by a ca 1 000 m long 8"1/2 subhorizontal drain drilled under a LWD (Logging While Drilling) – MWD – RSS (Rotary Steerable System) – BHA (Bottomhole Assembly). The latter avoided the sliding (non rotating) and hole geometry control episodes inherent to conventional MWD x PDM directional drilling methods, thus achieving substantial time savings and upgraded hole calibration.

Low density (<1.1 SG) (brine) water based and biopolymer mud formulations were circulated while drilling the reservoir 8"1/2 drilling phase.

Class G cement slurries (densities varying from 1.60 to 1.90 SG) were used and stage cementing procedures operated whenever needed (10"3/4 casing phases). Cement bonding and annular channeling were checked by means of current CBL-VDL and USI-IBC cased hole logging tools.

SH drains were not completed and left as openhole, owing to the consolidated structure od the carbonate reservoir rock mass.

4. DRAIN NAVIGATION. GEOSTEERING STRATEGY

The key idea behind the geosteering workflow while drilling the SH drains, consists of matching the productive (net pay) sequence thanks to relevant porosity indicators interacting with the navigation process, which are sourced by LWD, drilling parameters (rate of penetration, ROP, torque…), offset wells and real time (0.5 hour delayed respective to bit progress) geochemical (XRF and XRD) ratios.

It involves a two stage process flowcharted in Figure 5 summarised here after (Ungemach et al, 2018; Di Tommaso et al, 2018):

While drilling. Integrated, real time, geosteering data acquisition;

Directional drilling: monitor and control RSS downhole tool performance;

LWD tool string: Gamma Ray, Neutron porosity, multi frequency resistivity, (imaged) azimuthal density;

XRD, XRF: XRay Difractometry and Fluorescence for mineralogic and elemental analysis;

Mud logging: cutting petrography.

Post drilling analysis.

Integration of Wireline Nuclear Magnetic Resonance (CMR tool) and Dipole Sonic (DSI tool) for matching drain productive segments;

Production Logging Tool (PLT) and micro-spinner flowmetering providing flow and temperature profiles along the entire openhole (OH) drain.

The exercise on the first (GCAH1) well is illustrated in Figure 4. Here, after selecting, via Gamma Ray/Neutron log squaring, the most representative offset well, the producing layers were tracked over the whole pay zone to identify precisely the production layering sequence.

The XRD/XRF geochemical monitoring results and expectations are depicted in Figure 6 and commented, with respect to (i) the candidate alkaline (Sr, Na, Mg) and mineral (Mn, Fe, Zn) proxies as porosity and diagenetic markers respectively, and (ii) metal oxide marine littoral (carbonate barrier) lithofacies indicators (Brand and Veizer, 1980).

The data set and experience gained on well GCAH1 were integrated into the geosteering of (injector) well GCAH2, which addressed a more complex reservoir and structural setting, characterised by a poorly porous/pervious reservoir and fast varying up dipping trend.

The complexity of the RSS navigation process is imaged in Figure 7, which evidences the many corrections implied in securing the trajectory within the two thin bedded porous intervals.

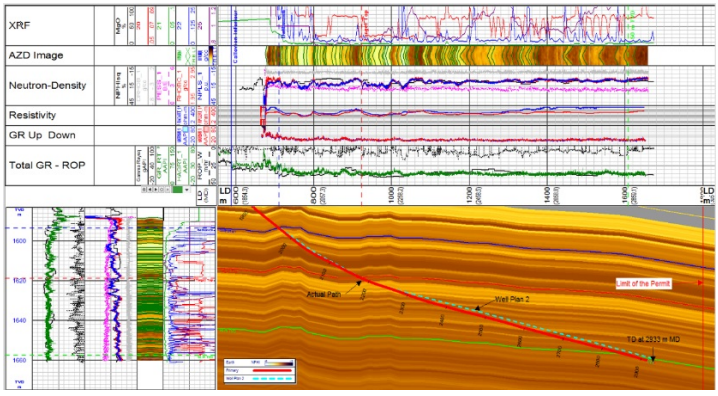

Figure 4: Well GCAH1. Drain trajectory guidelines

- Select a reference offset well for correlating neutron/density logs.
- Track productive layers according to flowmeter logs of nearby wells and intersect entire the pay interval.

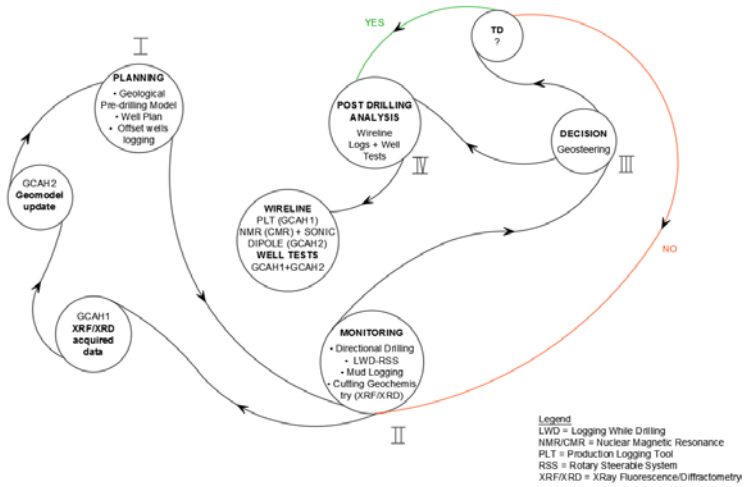

Figure 5: Geosteering workflow chart

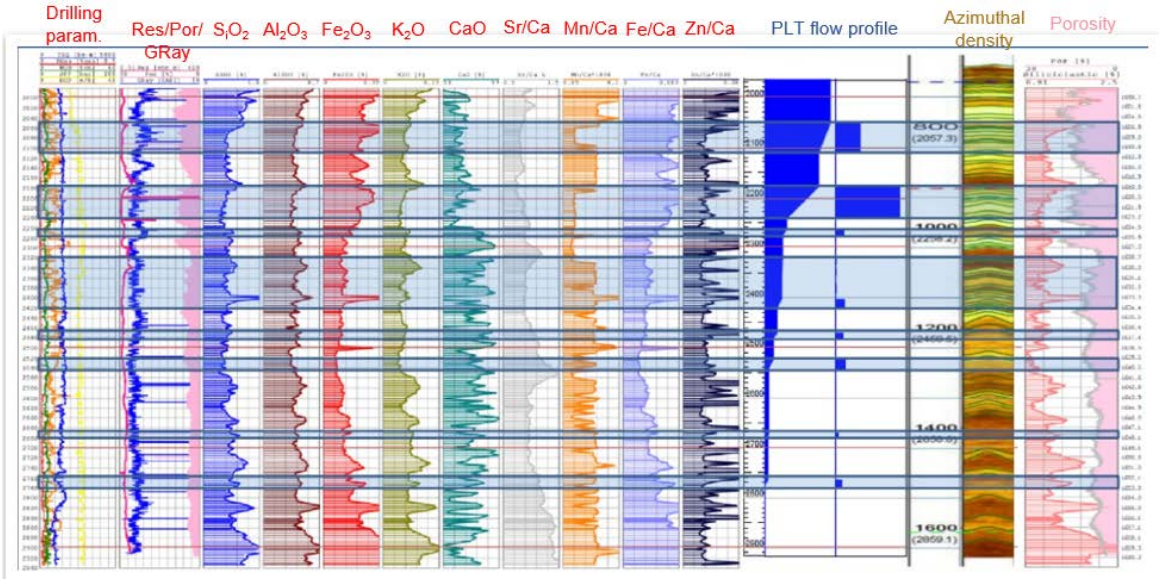

Candidate proxies

According to U. Brand and J. Veizer (1980), in carbonates diagenetic equilibration Sr^{+2}, Na^{+2} and Mg^{+2} decrease, while Mn^{+2}, Fe^{+2} and Zn^{+2} increase

Sr, Na, Mg ← Porosity / Diagenetic Degree → Mn, Fe, Zn

- Objective. Correlate, geochemical traced, lateral carbonate variations with LWD data to optimise GCAH2 geosteering.
- Identify diagenetic, cement, microfracturing shows impacting porosity.
- Put these figures in perspective with PLT flowmetering while designing GCAH2 trajectory.

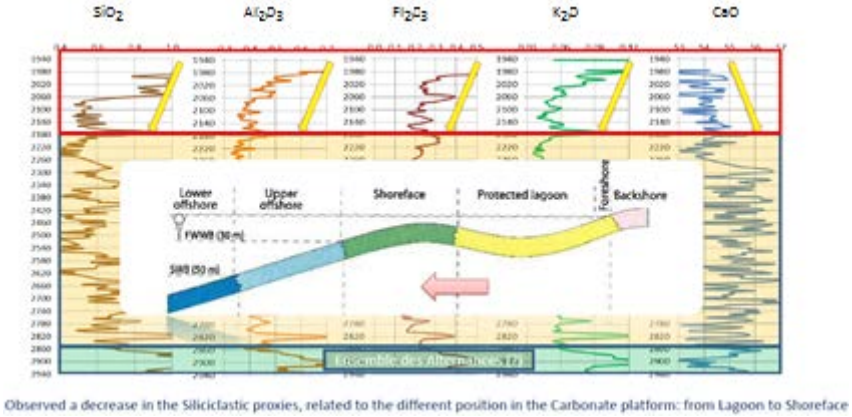

Observed a decrease in the Siliciclastic proxies, related to the different position in the Carbonate platform: from Lagoon to Shoreface

Siliciclastic proxies. Carbonate platform environment

Figure 6: Well GCAH1. Geochemical XRF, XRD monitoring

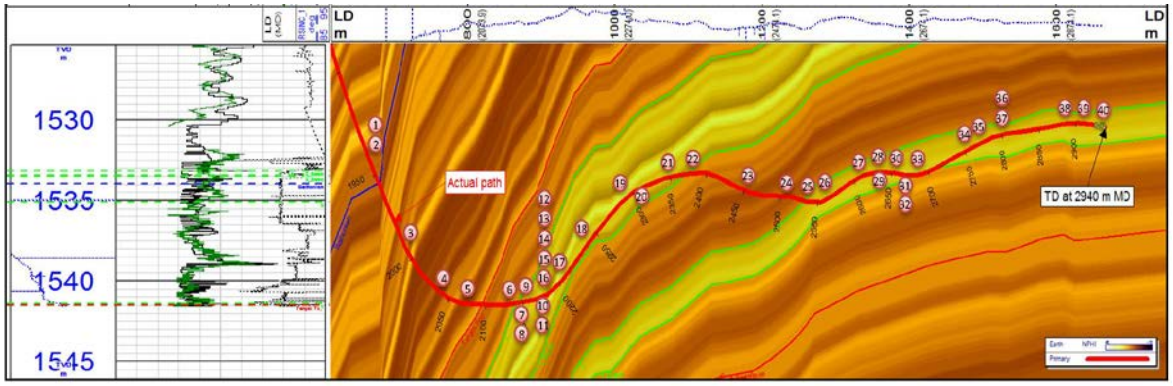

CRITICAL CASES

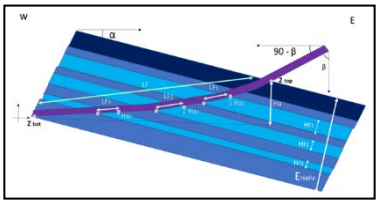

α=1° ß=88° Actual E=60m Then:	Well architecture similar to GCAH1 which has intersected the whole payzone	α=5° ß=88°3 Actual E=20m Then:	After crossing the entire pay interval will drilling progress upwards?

- Challenge: Real time trajectory corrections
  - 1 to 5° varying dips, impacting drain effective length
  - Reconcile tracking of thin (#1 m) high porosity layers with target matching delays induced by high bit to RSS recording distance (#20 m)

Figure 7: Well GCAH2. Geosteering. Trajectory corrections

5. FORMATION EVALUATION

Well assessment of reservoir and well performance was carried out via (i) wireline (openhole, PLT) logging, (ii) well testing, (iii) heat and mass transfer modelling, and (iv) geochemical monitoring.

5.1 Wireline Logging

The ambitioned exhaustive wireline logging programme initially contemplated could not be wholly fulfilled owing to tractor drive limitations and got therefore restricted to the set of logs listed in Table 1.

However, respective to porosity, density and lithology, logging while drilling (LWD) supplied useful clues while geosteering drain trajectories, particularly on well GCAH2 characterised by a thin metric size, (up) dip varying, bed structure exemplified in Figure 9.

On well GCAH1, the successful PLT spinner flowmetering provided unvaluable information as to the flow and dynamic temperature profiles along the entire drain path (Figure 8). This key information enabled to assign a (flow weighted averaged) formation temperature and calibrate a wellbore heat transfer model in order to match monitored wellhead temperatures and derive accordingly a well discharge vs surface temperature function, indeed a critical issue in forecasting future doublet heat delivery, an aspect discussed later in the modelling section.

Identification of drain productive segments is imaged in (GCAH2) composite log displayed in Figure 9.

On the other hand, the first application on French geothermal projects of nuclear magnetic resonance (NMR/CMR) and dipole sonic logs (Figure 10), proved rewarding and of great significance in correlating permeabilities to porosities and *vice versa*, along with assessing thin bed porosity layering and lateral extents from P and S wave sources, an exercise requiring advanced acoustic processing.

Given the significant input of the foregoing, combined NMR/CMR, dipole sonic and density wireline logs should become soon a standard in assessing well/reservoir performance, geomechanical properties and related well wellbore stability issues.

Table 1 : Wireline logging (completed) programme

LOG TYPE	LOGGING TOOL	DRILLING PHASE(")								CASING PHASE(")					
		26		18"1/2		14"3/4		8"1/2		20		16		10"3/4	
		GCAH1	GCAH2	GCAH1	GCAH2	GCAH1	GCAH2	GCAH1	GCAH2	GCAH1	GCAH2	GCAH1	GCAH2	GCAH1	GCAH2
LWD	GR														
	Density/AZD														
	Neutron														
	Resistivity														
OH	GR														
	CAL(BGL)/XY														
	Density														
	Neutron														
	Sonic (2P)														
	NMR														
	XRDF/XRF														
CH	IBC/USI														
	CBL-VDL														
	CIC (MAC60)														
PLT	FS														
	FM (Spinner)														
	QPG, PTMG														

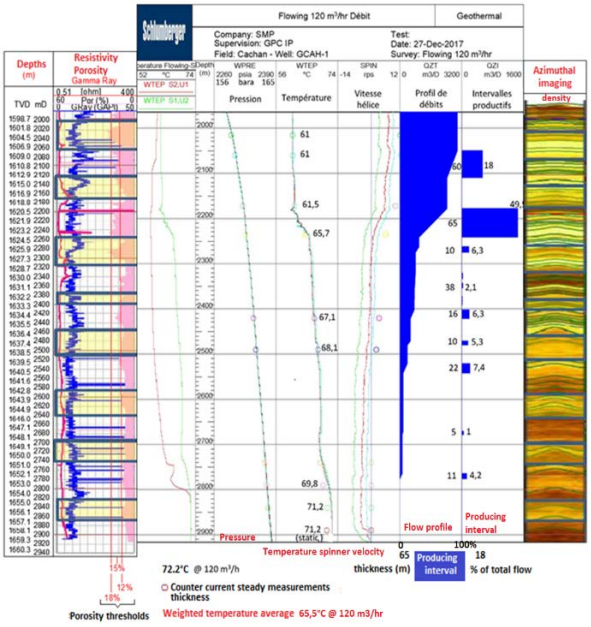

Figure 8 : Well GCAH1. PLT logging. Flowmetering, temperature and pressure logging of the openhole subhorizontal drain (27/12/2017). Co-current dynamic measurements

Table 2 : Well test summary

Test type	Well		Objective
	GCAH1	GCAH2	
Self flowing step drawdown production.			
• prior to acidising	X	X	Raw PI
• post acidising	X	X	Stimulated PI – Acidizing efficiency
Self flowing, constant flowrate production.			Reservoir/subhorizontal drain evaluation (transmissivity, permeability, acrisotropy skin)
• pressure drawdown	X	X	
• pressure build up	X	X	
Sustained, variable flowrate injection.			
• step drawdown		X	(Stimulated) II
• pressure rise		X	Reservoir/subhorizontal drain injective performance
• pressure fall off		X	

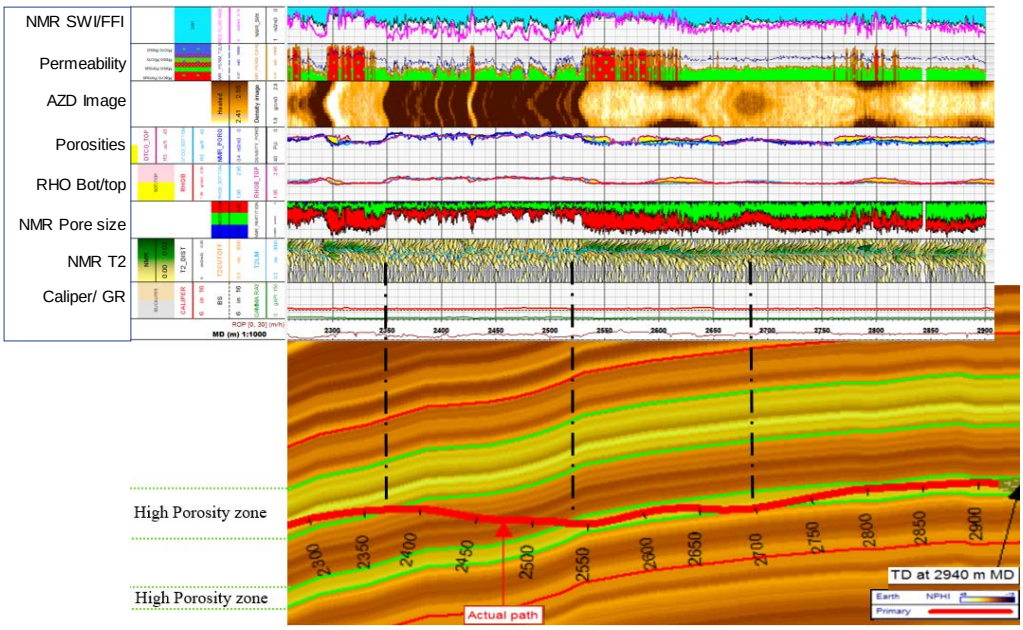

Figure 9: Composite permeability, porosity, density log imaging of a subhorizontal drain (well GACH2) (source: Cavalleri and Wielemaker, 2018)

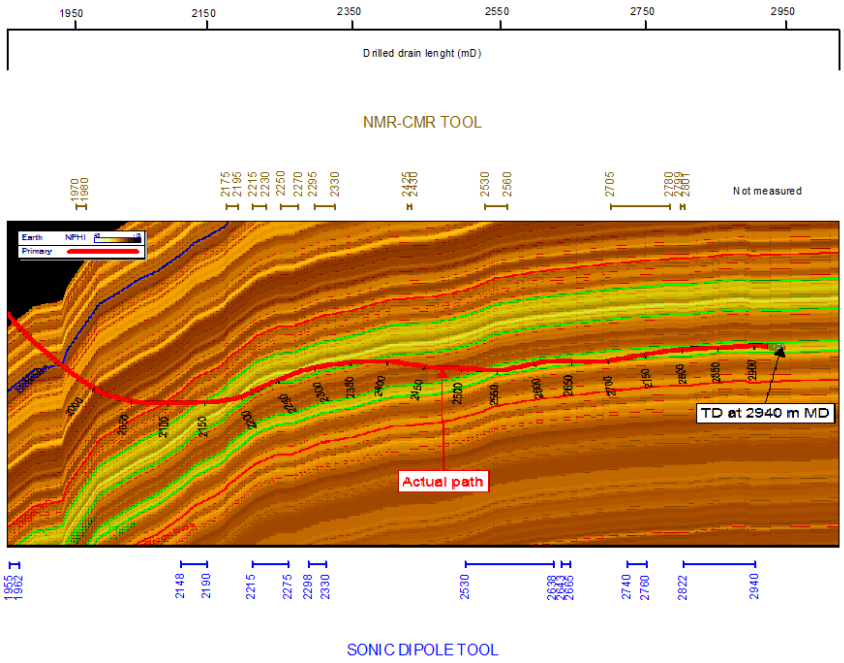

Figure 10: Well GCAH2. Wireline log (NMR-CMC and Sonic Dipole porosity, permeability tools) correlation with drain productive segments

5.2 Well Testing

Well tests were performed according to the programme summarized in Table 2, which included three types of transient test sequences (i) step drawdown production tests, (ii) production drawdown and build up on both wells, and (iii) injection step rise and fall off (on well GCAH2) in order to assess well delivery/injecting capacities and SH drain/reservoir performance.

It should be readily pointed out that in no way were transient well test analysis and interpretation an easy exercise, as a consequence of a local reservoir environment characterised by (i) a stratified structure intercepted by a subhorizontal, occasionally tortuous, drain trajectory, (ii) a non homogeneous flow distribution along the drain, (iii) interlayer crossflow, dramatically amplified by weak (self-flowing) production capacities as a result of limited waste fluid evacuation facilities, and (iv) pressure, and temperature interferences induced by neighbouring GDH doublets operating in winter season at maximum flow ratings.

The foregoing obviously strongly impacted and complicated test operation and interpretation, the latter strongly inspired by horizontal transient well test analysis (Lee et al, 1982).

Tests were carried out after due, coiled tubing operated, acid stimulation over the, log selected, productive drain segments, whose benefits on productivity indices (PIs) stand as follows.

Well	GCAH1	GCAH2
Pre acidising	- (*)	21
Post acidising	41.5	38

(*) test stopped (waste disposal pump failure)

The geometry of an idealised, laterally and vertically bound, horizontal drain and related transient flow regimes are illustrated in Figure 11 (idealised, time dependent, pressure and pressure derivative patterns), which, identifies five distinctive flow regimes and their signatures on the pressure and pressure derivative plots, from early to late times, (i) wellbore storage, (ii) early radial, (iii) early linear, (iv) pseudo-radial, and (v) late linear.

However and whatever the local testing contraints, Figure 12 shows, on the pressure derivative related to production well GCAH1, a good match with the early radial and pseudo-radial drainage modes (zero slope plateau) enabling, according to Lee et al (1982), the application of conventional interpretation methods by the semi-log MDH and Horner plots, which clearly exhibit straight line segments in their terminal (late recovery time) sections. Transmissivities were derived accordingly, leading to a Horner value close to 30 Dm. No direct derivation of the skin factor was attempted so far, given the drain geometry and multilayered reservoir structure not to mention the assignment of a relevant permeability value. An indirect path was therefore followed, which consisted of deriving, from the well delivery curve, an equivalent transmissivity integrating the true calculated transmissivity (# 30 Dm) and the skin factor, the latter calculated by matching computed to measured pressures, resulting in a skin factor S = -3.5.

An alternative method was later investigated by calculating the drain productivity index PI, following the method suggested by Economides et al (1996), which addresses a horizontal drain equidistant from reservoir boundaries, an approach developend in Appendix 1, which leads to a PI=39 m^3/h/bar, a figure which stands close to the measured value.

On well GCAH2, injection testing could be performed, contrary to well GCAH1 production tests, at higher sustained flow ratings thanks to the availability of two on site injection well pumping facilities, diverted for the purpose to the newly completed well GCAH2 enjoying therefore a 350 m^3/hr rated capacity. Well injective performance is depicted in Figure 13.

Summing up, well transmissivities, skin factors and productivity/injectivity indices shape as follows.

Well	Transmissivity (Dm)	Skin factor	PI, II (m^3/hr/bar)
GCAH1	28	-3.5	PI=41.5
GCAH2	30	-4.5	II=28

Gains achieved on well transmissivities measured on existing wells stand at two (GCAH1) and 3 (GCAH2), thus validating the SHW concept.

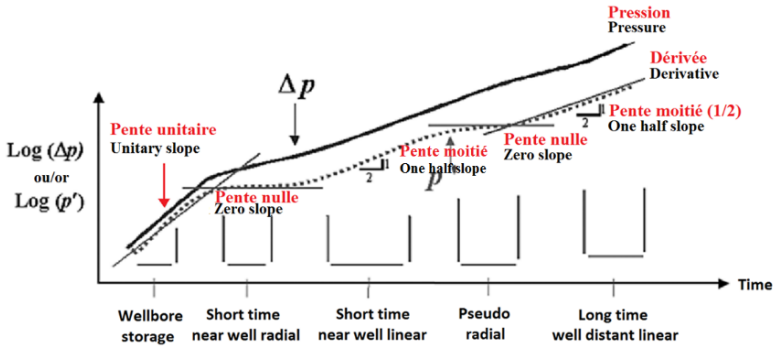

Figure 11: (Sub)horizontal drain (idealised) flow regime identification (after Lee et al, 1982)

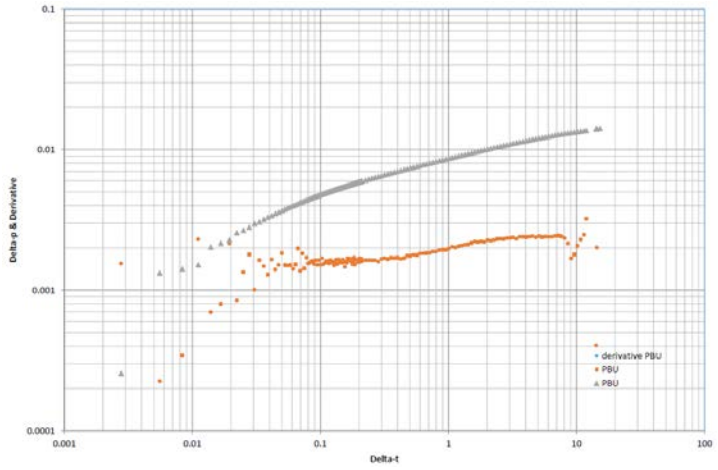

Figure 12: Well GCAH1. Self flowing production test. Build up pressure and derivative log-log plots

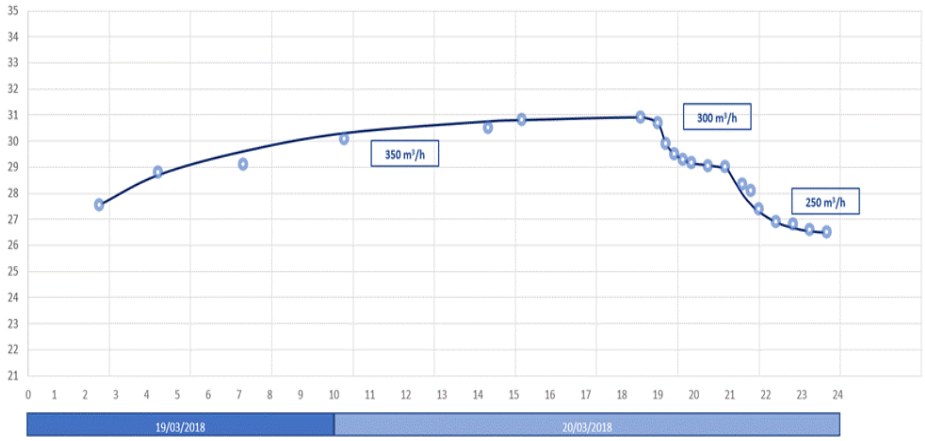

Figure 13: Well GCAH2. Step rise injection test. Well injectivity curve.

5.3 Modelling

Three modelling issues were addressed (i) well test modelling, (ii) wellbore heat transfer modelling, and (iii) reservoir simulation of present status and future predicted, pressure and temperature patterns, respectively.

A satisfactory fit was achieved in reproducing the recorded bottomhole pressures in response to a busy local (Cachan and neighbouring GDH doublets) production/injection history, adding to a varying GCAH1/GCAH2 production testing schedule proper. Hence, the simulation exercise, based on TOUGH2 (Pruess et al, 1999), m-View interfaced, heat and mass transfer software, and on the multilayered sandwich equivalent reservoir structure (Antics et al,2005) illustrated in Figure 14, validated the, test issued, input reservoir hydrodynamic parameters.

Calibrating a well heat transfer module became soon an urgent concern, aimed at predicting future well head vs bottomhole temperatures as a function of flowrates. The wellbore heat transfer model was able to match the monitored wellhead temperatures from the, PLT derived, bottomhole temperature. From there on were anticipated future wellhead temperatures as a function of bottomhole temperatures and production ratings. Assuming higher flowrates would cause bottomhole temperatures to rise and, consequently, a 450 m^3/h target production flowrate and time would lead to a wellhead temperature nearing 70°C thus minimising conduction losses ($\leq$ 0,5°C).

Once calibrated, the reservoir simulation module could infer the pressure interferences induced by the GCAH1-GCAH2 subhorizontal doublet operating at maximum flowrate on the nearby GDH doublets, an exercise, exhibiting minimum if not negligeable impacts.

Predictive model runs were further extended to forecast the temperature cooling and pressure depleting/rising trends 30 years ahead (until year 2048); results, mapped in Figure 15 (maximum cooling and depleted areas in year 2048), are deemed to validate the future exploitation schedule.

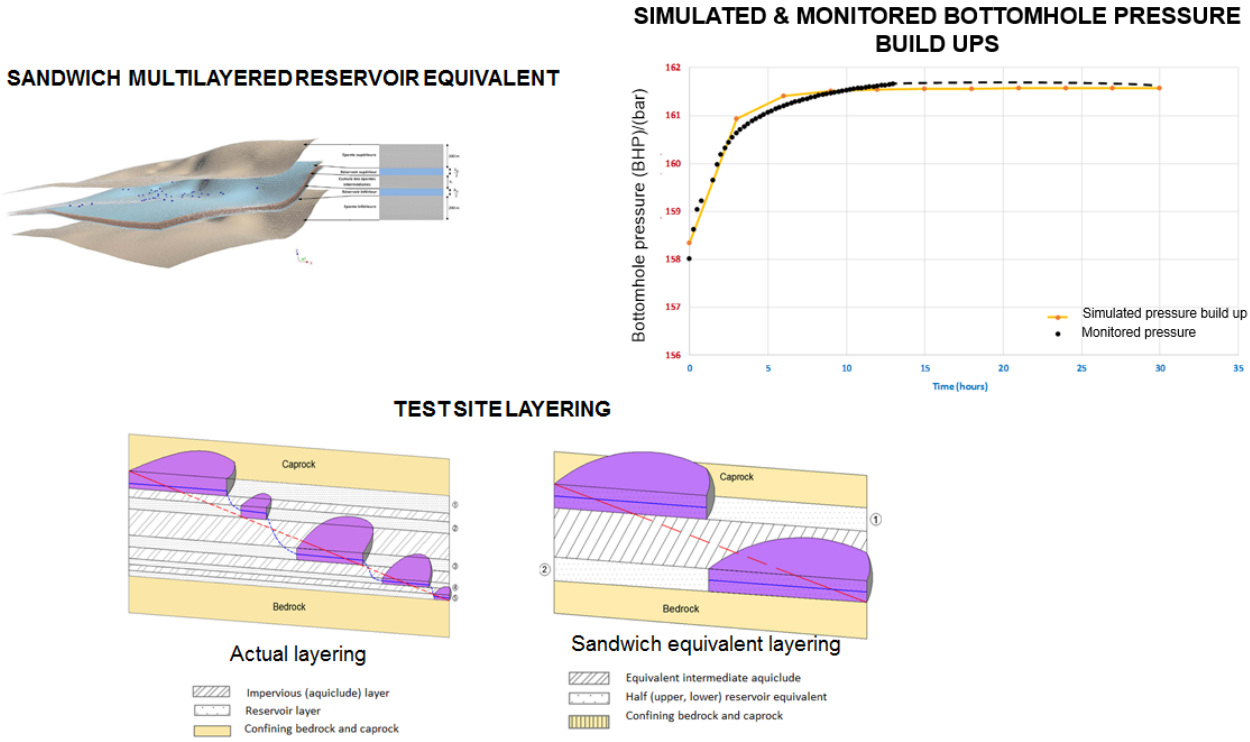

Figure 14: Subhorizontal drain modelling. Flow model, pseudo radial stationary, typology

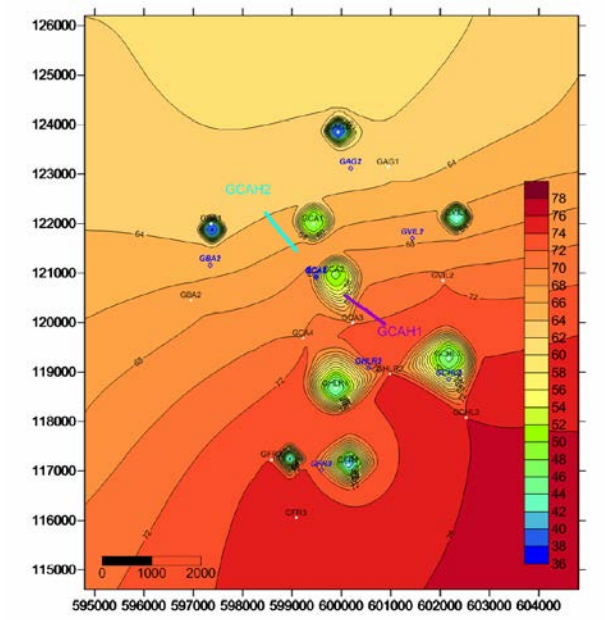

Figure 15.a: Cold bubble and pressure depletion map

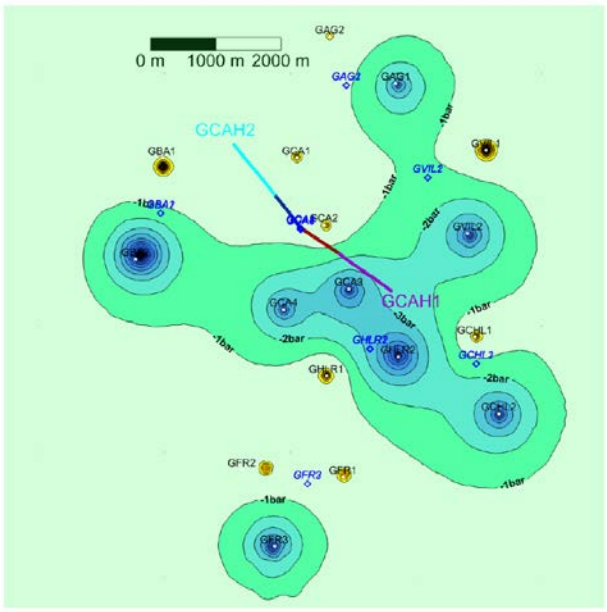

Figure 15.b: Maximum winter pressure drawdowns

Figure 15: Simulated pressure and temperature patterns (year 2048)

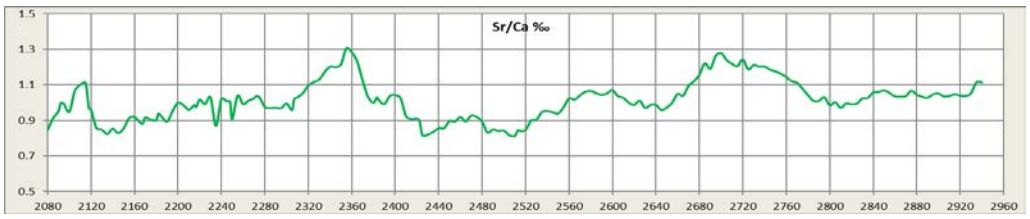

Sr/Ca plot highlighting the (0.7-1.1‰) interval

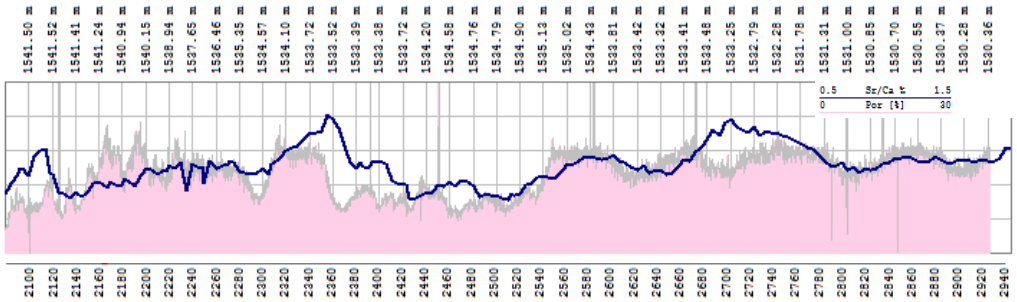

Correlation between raw Porosity log and Sr/Ca

Figure 16: Well GCAH-2. Sr/Ca ratio and LWD raw (neutron & density) porosity correlation

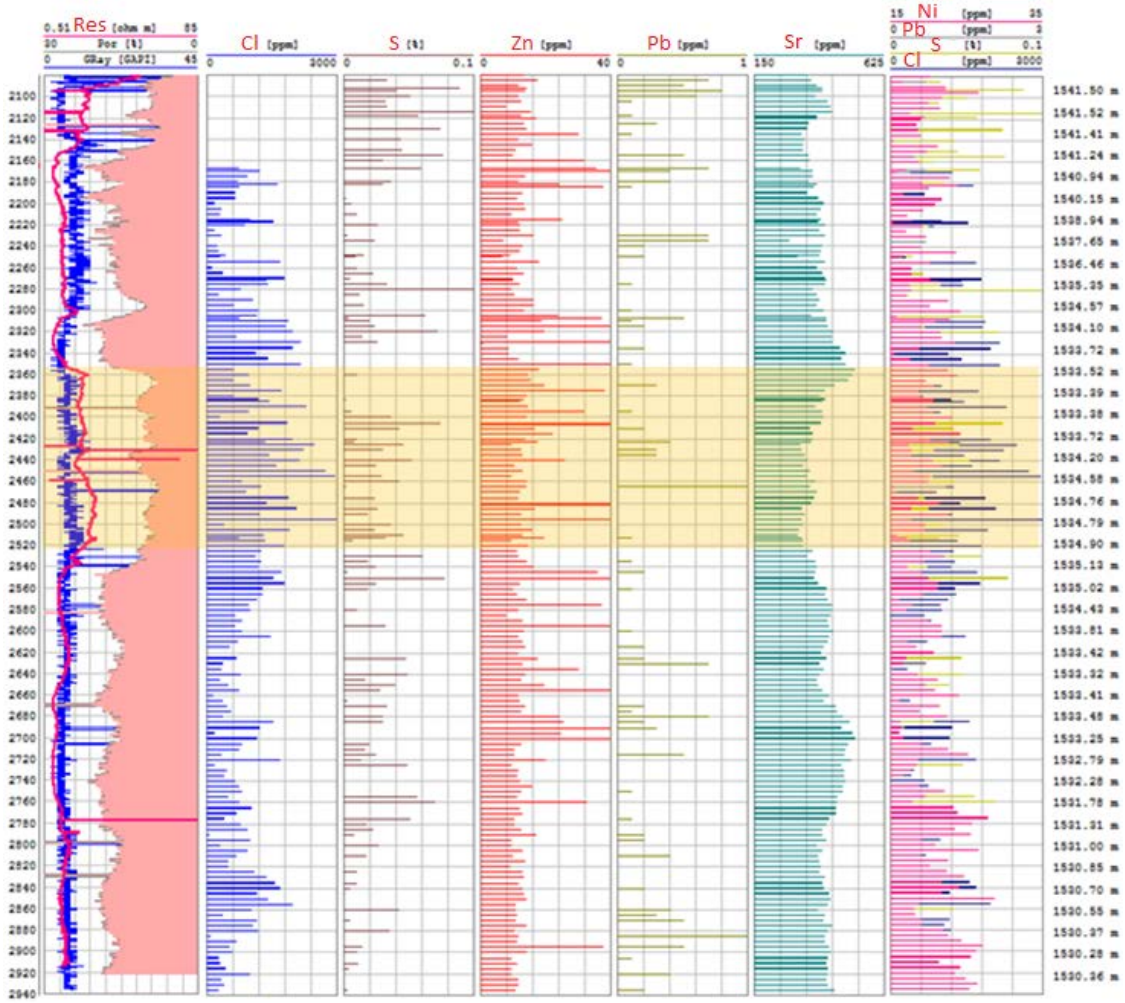

Figure 17: Well GCAH-2. Positive anomalies in micro-fracture markers. Colored band corresponds to the [2360-2530 mD] low porosity cemented interval

(source: Geolog & GPC IP, 2018)

5.4 Geochemical monitoring

Within the context of the Paris Basin Dogger carbonate platform, geochemical monitoring, based on XRF (X Ray fluorescence) elemental and XRD (X Ray diffractometry) mineralogic analyses on cuttings, sampled while drilling, was implemented with a view to appraise varying reservoir properties in response to facies changes and diagenetic impacts on porosity/permeability trends.

Hence, the process targeted three main objectives:

(i) Carbonate vertical and lateral reservoir zonation and depositional environments by correlating LWD (neutron and azimuthal density, AZD) with XRF issued elements and XRD derived mineralogies, which, once characterized on well GCAH1, would serve as markers for optimizing well GCAH2 trajectory;

(ii) Evaluation of rock petrography from porosity assessments, inferred from diagenesis and cement occurrence (Moore and Drucksman, 1981), (Brand and Veizer, 1980);

(iii) Microfracturing detection by tracking filling minerals through minor and trace element concentrations regarded as indicators, of microfracture aperture (open) and sealing (closed) (Moore and Drucksman, 1981) elsewhere supported by LWD (and mud logging) evidence.

• *Depositional environments*

From the three identified lithostratigraphic units, from top to bottom (i) Comblanchien, (ii) Oolites, and (iii) Alternances identified on both wells, only the two first quoted exhibit reservoir properties (i.e. LWD neutron porosities in the 15-20% range). The first depositional setting relates to the internal part of the lagoon (i.e. the shallower platform level) and the Oolitic limestones to a barrier (infralittoral) type (i.e. the transition from the internal, lagoon – part to the external – barrier – part of the carbonate platform).

• *Selected markers (oxides, elemental ratios, proxies)*

Salient features respective to sedimentary unit characterization, carbonate, diagenesis and porosity markers are portrayed as XRF oxides ($Si\ O_2$, $Al_2\ O_3$, $Fe_2\ O_3$, $K_2\ O$ and Ca O), plots, [Sr/Ca] and [Mn, Fe, Zn, Ca normed] ratios and summed siliciclastic [$\sum$ ($Si\ O_2$ + $Al_2\ O_3$ + $Fe_2\ O_3$ + $K_2\ O$)] proxies.

A quite remarkable correlation, exemplified in Figure 16, between the Sr/Ca ration and LWD neutron porosity can be noticed within the (0.9-1.1%) range.

• *Microfracturing indicators*

Worth to mention is the distinctive positive anomaly of N_i, Pb and S concentrations limited to the (2360-2530 mMD) interval, noticed on Figure 17 (well GCAH2); it happens to match precisely the non productive section of the drain, thus confirming their contribution as a micro-fracture (in this instance cemented) indicator.

6. CONCLUSIONS

There is clear evidence the project achieved technical and economic viability of the subhorizontal well concept in a multilayered reservoir sedimentology setting and densely populated urban and drilling environments.

Actually, the following doublet, existing vs future, performances speak for themselves.

Status	Doublets	Flow & energy ratings	COP	Mining CAPEX
Existing	2	350 m^3/hr; 40 GWh_{th}/yr	9	14-15 Mio €
Future	1	450-500 m^3/hr; 60-65 GWh_{th}/yr	20-28	12-13 Mio €

Lessons learned have highlighted:

(i) the RSS/PDC bit directional drilling prerequisite, securing fast penetration rates, improved trajectory control and hole calibration among others. The availability of a RSS designed BHA for the 14"$^{3/4}$ phase would have significantly impacted drilling and trajectory monitoring performance;

(ii) the benefit, exemplified on well GCAH2, of a multidisciplinary, geosteering team approach, combining drilling, logging, geological, reservoir engineering, geochemical skills and expertise;

(iii) the efficiency of a well stimulation protocol mobilizing a 1"$^{3/4}$ to 2" Coiled Tubing facility and large acid (HCl, 15X) amounts (up to 200 m^3, well GCAH2) allowing to selectively spot the acid on drain segments selected from LWD and OH porosity (and porosity/permeability) wireline information;

(iv) the significant input of the combined NMR/CMR, dipole sonic and density wireline logging segment suggests they become a standard in assessing well/reservoir performance, geomechanical properties and wellbore stability issues;

(v) well testing sequences, although limited in time (maximum 45 hrs), matched satisfactorily horizontal transient well test theory and related time dependent phases exhibited by pressure derivative plots, and

(vi) last but not least, real time geochemical monitoring via XRF and XRD, elemental and mineralogic analyses on sampled cuttings, provided rewarding clues with respect to selected (oxides, elemental ratios, proxies) porosity markers and related diagenetic and micro-fracture indicators.

In future designs of subhorizontal (or multiradial) well architectures, due attention should be paid to (i) cementing procedures and protocols favouring stage cementing of the 10"$^{3/4}$ and 16" sections, (ii) accommodate hole transition from the 10"$^{3/4}$ cased/cemented to the 8"$^{1/2}$ OH drain sections in order

to ease the passage of long, tractor driven, OH/PLT wireline, logging strings, (iii) elaborate relevant geosteering strategies, based on either (or both) careful screening of candidate documented offset wells and descending (reconnaissance)/ascending (optimizing) drain trajectories within the identified pay interval, and (iv) longer (up to 120 hrs) well testing sequences so as to best appraise long term drain hydraulic behaviour in relation to lateral/vertical boundary and anisotropy effects, and interlayer cross flow artefacts.

7. ACKNOWLEDGMENTS

The authors with to than DALKIA (EDF Group), project owner, and the city of Cachan, project initiator, for authorizing to publish this paper. Their thanks extend to the French Environmental Agency, ADEME, which, along with the Ile-de-France Region, has significantly contributed to project funding the drilling supervision staff, geosteering team, XRF/XRD unit and wireline logging champions.

REFERENCES

Antics, M., Papachristou, M., and Ungemach, P. (2005). Sustainable Heat Mining. A Reservoir Engineering Approach. Proc. *Thirtieth Workshop on Geothermal Reservoir Engineering*. Stanford University, CA, Jan.31-Feb. 2, 2005.

Brand, U., Veizer, J. (1980). Chemical Diagenesis of a multicomponent Carbonate System. 1 Trace Elements. J. of Sedimentology Res.**50** (4), 1219-1236.

Bruel.D. (2008). Etude du Potentiel de l'Aquifère du Dogger en Région Parisienne Exploité à l'Aide de Forages à Déport Horizontal. Rapport Mines de Paris Tech No R081031 DBRU.

Cavalieri, C., and Wielemaker, E. (2018). Wireline NMR Combined with Azimuthal Logs to Define Flow Capacity and Homogeneity within High Angle Geothermal Well. First EAGE/IGA/DGMK Joint Workshop on Deep Geothermal Energy. Strasbourg, 8-9 Nov.2018.

Cavalleri, C., Wielemaker, E. (2018). Wireline NMR Combined with Azimuthal Logs Define Flow Capacity and Homogeneity within High Angle Geothermal Well. SPWLA France. Technical Session, Paris/SGF, 27 nov. 2018.

Economides, M.J., Brand, C.W, Frick, T.P, (1996). Well Configurations in Anisotropic Reservoirs. SPE Formation Evaluation paper SPE27980, Dec. 1996.

Appendix 1: Productivity index of a horizontal drain

We refer here to the M.Economides et al (1996) approach, quoted by J.Lee et al (2002), who consider a horizontal drain, equidistant from the reservoir, assumed homogeneous and isotopic, boundaries, an approach preferred to that of Babu and Odeh (1988).

Frieg, B. (2014). Access to the Hydrothermal Reservoir of the Upper Muschelkalk Formation at Schlattingen in the Canton of Thurgau (Northern Switzerland). Deep Geothermal Days; Conference, Exhibit and Workshop, Paris, 10-11 April, 2014.

Hill, A.D., Zhu, D., and Economides, M.J. (2008). Multilateral Wells. Soc. Pet. Eng., Richardson, TX, USA.

Lee, M.J., Rollins, J.B., and Spivey, J.P (1982). Pressure Transient Testing, chapter 12 Horizontal Well Analysis. SPE Textbook Series, vol.9, Henry L. Doherty Memorial Fund of AIME, Richardson, TX, USA.

Promis, M.P., Ungemach, P., and Antics, M., (2013). Subhorizontal Geothermal Well Completion. A Promising Outlook. Proc. European Geothermal Congress. EGC 2013. Pisa, Italy, 3-7 June, 2013.

Pruess, K., Oldenburg, C.M, and Moridis, G. (1999). TOUGH2 User's Guide, Version 2.0, Lawrence Berkeley, CA, USA.

Ungemach, P., Antics, M., P., Borozdina, O., Foulquier, L., and Papachristou, M. (2011). Geomodelling and Well Architecture, Key Issues to Sustainable Reservoir Development. Proc. *Thirty-Sixth Workshop on Geothermal Reservoir Engineering*. Stanford University, Stanford, CA, USA, Jan.31-Feb. 2, 2011.

Ungemach, P., Antics, M., and Promis, M.P. (2016). Extended Reach Wells for Enhanced Heat Production. Proc. *European Geothermal Congress, EGC 2016*, Strasbourg, France, 19-24 Sept.2016.

Ungemach, P., Antics, M., Davaux, M.,Di Tommaso, D., Moosavi, S., and Casali, F. (2018). Real Time Geosteering Integrated Services. A Key Issue in Maximizing Geothermal Exposure and Minimizing Drilling/Completion Risk. A Paris Basin Case Study. Celle Drilling International Conference and Exhibition for Advanced Drilling Technology, Celle, Germany 11-12 Sept.2018.

www.thinkgeoenergy.com. Project completes first subhorizontal geothermal well near Paris, 4 Jan;2018. Geothermal project near Paris successfully completes 2nd subhorizontal well; 20 March.2018.

$$PI = \frac{4{,}86\ 10^{-3}\ k^{*}(md)\ b_H\ (m)}{\mu\ (cp)\quad \left[P_D + \frac{b_H(m)}{2\ \pi\ L_d(m)}\ \Sigma S\right]}$$

where:

$$P_D = \frac{b_H}{2\pi}\left[\frac{C_H}{2h} + \frac{S_c}{L_d}\right] \qquad k^* = kx = ky = kz$$

$$S_c = \mathrm{Ln}\left(\frac{h}{2\pi r_d}\right) - \frac{h}{6L_d} + S_e$$

$$S_e = \frac{h}{L_d}\left[\frac{2dz}{h} - \frac{1}{2}\left(\frac{2dz}{h}\right)^2 - \frac{1}{2}\right] - \mathrm{Ln}\left[\sin\left(\frac{\pi d_z}{h}\right)\right]$$

with:

S = O (zero offset along the vertical axis)

C_H = shape coefficient in the horizontal plane (see Table 1)

Observation:
Case of an anisotropic reservoir

- Lenghts
  $L'_d = L_d\ \alpha^{-1/2}\ ß$
- Radii
  $r'_d = r_d\ \frac{\alpha^{2/3}}{2}\left(1 + \frac{1}{\alpha ß}\right)$

with:

$$\alpha = \sqrt{\frac{(k_x k_y)^{1/2}}{k_z}} \qquad ß = \left(\sqrt{\frac{k_x}{k_y}}\cos^2\rho + \sqrt{\frac{k_y}{k_x}}\sin^2\varphi\right)^{1/2}$$

φ : trajectory azimuth along the oy axis

$x' = x\left(\sqrt{k_y\, k_z / k^*}\right)$;

$y' = y\left(\sqrt{k_x\, k_z / k^*}\right)$; $\qquad z' = z\left(\sqrt{k_x\, k_y / k^*}\right)$

$k^* = (k_x\, k_y\, k_z)^{1/3}$

Numerical application (see well) and reservoir geometry in Figure 1.

$b_H = a_H = 1\,000$ m

$L_D = 350$ m (drain productive length)

h = 10 m

$r_d = 0.108$ m

$C_H = 2.21$ (cf. Table 1)

$k^* = k_x = k_y = k_z = 1\,000$ mD

μ = 0.45 cp

∑ S (skin) = -3.5

leads to a PI of 39 m^3/h/bar, a figure which stands close to the measured value.

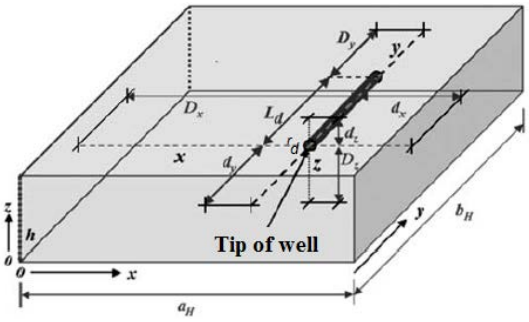

Figure 1: Well and reservoir geometry for a horizontal well

Table 1 : Shape coefficients (horizontal plan)

		L_W/b_H	C_H
b_H / L_W / a_H	$b_H = 4a_H$	0.25	3.77
		0.5	2.09
		0.75	1.00
		1	0.26
	$b_H = 2a_H$	0.25	3.19
		0.5	1.80
		0.75	1.02
		1	0.52
	$b_H = a_H$	0.25	3.55
		0.5	2.21
		0.75	1.49
		1	1.04
	$2b_H = a_H$	0.25	4.59
		0.5	3.26
		0.75	2.53
		1	2.09
	$4b_H = a_H$	0.25	6.69
		0.5	5.35
		0.75	4.63
		1	4.18
b_H / L_W / a_H	$b_H = a_H$	0.25	2.77
		0.5	1.47
		0.75	0.81
		1	0.46
b_H / L_W / a_H	$b_H = a_H$	0.25	2.66
		0.5	1.36
		0.75	0.69
		1	0.32
		θ	
b_H / L_W / θ / a_H	$b_H = a_H$ $L_W/b_H = 0.75$	0	1.49
		30	1.48
		45	1.48
		75	1.49
		90	1.49